The Oncologist®

Radiation Versus Immune Checkpoint Inhibitor Associated Pneumonitis: Distinct Radiologic Morphologies

Xuguang Chen [ID],[a] Khadija Sheikh [ID],[a] Erica Nakajima,[d] Cheng Ting Lin,[b] Junghoon Lee,[a] Chen Hu,[c] Russell K. Hales,[a] Patrick M. Forde,[d] Jarushka Naidoo,[d] Khinh Ranh Voong[a]

[a]Department of Radiation Oncology and Molecular Radiation Sciences, Johns Hopkins University School of Medicine, Baltimore, Maryland; Departments of [b]Radiology and Radiological Science, [c]Biostatistics, Oncology, and [d]Oncology, Johns Hopkins University, Baltimore, Maryland, USA
Disclosures of potential conflicts of interest may be found at the end of this article.

Abstract

Background. Patients with non-small cell lung cancer may develop pneumonitis after thoracic radiotherapy (RT) and immune checkpoint inhibitors (ICIs). We hypothesized that distinct morphologic features are associated with different pneumonitis etiologies.

Materials and Methods. We systematically compared computed tomography (CT) features of RT- versus ICI-pneumonitis. Clinical and imaging features were tested for association with pneumonitis severity. Lastly, we constructed an exploratory radiomics-based machine learning (ML) model to discern pneumonitis etiology.

Results. Between 2009 and 2019, 82 patients developed pneumonitis: 29 after thoracic RT, 23 after ICI, and 30 after RT + ICI. Fifty patients had grade 2 pneumonitis, 22 grade 3, and 7 grade 4. ICI-pneumonitis was more likely bilateral (65% vs. 28%; $p = .01$) and involved more lobes (66% vs. 45% involving at least three lobes) and was less likely to have sharp border (17% vs. 59%; $p = .004$) compared with RT-pneumonitis. Pneumonitis morphology after RT + ICI was heterogeneous, with 47% bilateral, 37% involving at least three lobes, and 40% sharp borders. Among all patients, risk factors for severe pneumonitis included poor performance status, smoking history, worse lung function, and bilateral and multifocal involvement on CT. An ML model based on seven radiomic features alone could distinguish ICI- from RT-pneumonitis with an area under the receiver-operating curve of 0.76 and identified the predominant etiology after RT + ICI concordant with multidisciplinary consensus.

Conclusion. RT- and ICI-pneumonitis exhibit distinct spatial features on CT. Bilateral and multifocal lung involvement is associated with severe pneumonitis. Integrating these morphologic features in the clinical management of patients who develop pneumonitis after RT and ICIs may improve treatment decision-making. *The Oncologist* 2021;26:e1822–e1832

Implications for Practice: Patients with non-small cell lung cancer often receive thoracic radiation and immune checkpoint inhibitors (ICIs), both of which can cause pneumonitis. This study identified similarities and differences in pneumonitis morphology on computed tomography (CT) scans among pneumonitis due to radiotherapy (RT) alone, ICI alone, and the combination of both. Patients who have bilateral CT changes involving at least three lobes are more likely to have ICI-pneumonitis, whereas those with unilateral CT changes with sharp borders are more likely to have radiation pneumonitis. After RT and/or ICI, severe pneumonitis is associated with bilateral and multifocal CT changes. These results can help guide clinicians in triaging patients who develop pneumonitis after radiation and during ICI treatment.

INTRODUCTION

Pneumonitis can cause significant morbidity or even mortality in patients with non-small cell lung cancer (NSCLC) after thoracic radiotherapy (RT) or immune checkpoint inhibitors (ICIs) [1, 2]. Computed tomography (CT) scans of the chest are critical in the diagnosis and management of patients with pneumonitis. Both RT- and ICI-pneumonitis can often manifest as ground-glass opacities (GGOs) and consolidations on CT, and both frequently assume a pattern of cryptogenic organizing pneumonia (COP) or acute interstitial pneumonia/acute respiratory distress syndrome (AIP/ARDS) [3–5]. However, it is unclear whether RT- and ICI-pneumonitis exhibit distinct radiographic patterns that would allow distinction of these two etiologies in patients with NSCLC. Moreover, CT morphology of pneumonitis after combined thoracic RT and ICI has not been systematically characterized.

The number of patients with NSCLC who may benefit from both thoracic RT and ICI is increasing [1, 6, 7]. As the indications for RT and ICI expand, more patients are at risk of developing pneumonitis after RT + ICI. Both RT and ICI may act synergistically to promote inflammation of the lung parenchyma, and several studies have suggested that prior thoracic RT is a potential risk factor for pneumonitis after ICI in a dose-dependent manner [8, 9]. However, studies of ICI-pneumonitis to date have mostly included heterogeneous patient populations with variable prior RT exposure [3, 4, 10, 11]. Furthermore, there are no universally accepted criteria to define the components of pneumonitis caused mainly by RT and that caused mainly by ICI [12]. Therefore, the respective roles of RT and ICI in pneumonitis pathogenesis among patients receiving RT + ICI remain unclear. This distinction is clinically relevant as treatment algorithms for RT-versus ICI-pneumonitis differ in that ICI-pneumonitis requires higher dose of steroids and occasionally immunosuppressive agents and may necessitate prolonged or indefinite discontinuation of ICI, which may have a negative impact on tumor control [2, 13–15]. We hypothesize that pneumonitis after RT + ICI may exhibit unique radiographic features compared with pneumonitis caused by either treatment alone. In this study, we compare CT characteristics of pneumonitis in patients with NSCLC after RT alone, ICI alone, or RT + ICI, using the framework proposed by Nishino et al. [3].

Compared with qualitative radiographic exam, CT radiomics may be able to discern subtle texture features not readily identified by human readers [16, 17]. In patients with NSCLC who receive RT or ICI, radiomic analysis of CT images combined with machine learning (ML) has shown promise in predicting future pneumonitis risk [18–21]. However, no study to date has evaluated the difference in radiomic signatures between RT- and ICI-pneumonitis. As a proof of concept, we aim to test the utility of CT radiomics (in place of morphologic evaluation) in discerning pneumonitis etiology by developing an unbiased, radiomics-based ML model and applying this model in patients who developed pneumonitis after receipt of RT and ICI.

MATERIALS AND METHODS

Patients

This study was approved by the institutional review board (IRB00218259). Patients with NSCLC treated at a single tertiary academic institution between 2009 and 2019 were retrospectively reviewed. Patients were included if they received curative-intent thoracic radiotherapy (≥45 Gy in 1.8–2.5 Gy per fraction) or ICI for any duration of time and developed pneumonitis. Patients who received ICI following thoracic RT after any interval were also included and classified as RT + ICI. Patients received regular follow-up with clinical and CT exams every 2 to 4 months for the first 2 years after treatment and every 3 to 6 months thereafter.

Baseline patient characteristics and treatment parameters were extracted from electronic medical records. Collected clinical variables included the age of initial diagnosis, gender, performance status, relevant comorbidities (smoking history, prior autoimmune disease, and chronic obstructive pulmonary disease [COPD]), baseline pulmonary function assessment (forced expiratory volume in 1 second [FEV1], forced vital capacity [FVC], and diffusion capacity of carbon monoxide), histology and stage of NSCLC at the time of initial diagnosis (American Joint Committee on Cancer, 7th edition), RT prescription dose, volume of lung receiving 20 Gy or higher (V20), mean lung dose (MLD), the type of ICIs, and additional treatments received (including RT to nonthoracic sites, chemotherapy, and prior surgery).

Pneumonitis Classification

Pneumonitis was diagnosed clinically by the treating physicians and defined as clinical and radiologic evidence of lung inflammation after RT or ICIs, not attributed to other confirmed causes such as active infection or progressive NSCLC [8]. Pneumonitis diagnosis in patients who received ICIs with or without prior RT was confirmed by a multidisciplinary group of physicians, including a medical oncologist, a radiation oncologist, a pulmonologist, and a radiologist in select cases. Time to pneumonitis was calculated from the date of RT completion in patients treated with RT alone, or from the date of ICI initiation in patients treated with ICIs alone or RT followed by ICIs. Grading of pneumonitis followed the Common Terminology Criteria for Adverse Events version 5.0.

CT Morphologic Evaluation

Diagnostic CTs before treatment initiation (pretreatment) and at the time of pneumonitis diagnosis (post-treatment) were obtained. Scanning parameters were listed in supplemental online Table 1. For patients who had multiple post-treatment CTs, the time point that showed maximal imaging changes was selected. Qualitative radiologic features as described by Nishino et al. were scored by a board-certified thoracic radiologist (C.T.L.) blinded to the patient's past treatment course and pneumonitis etiology [3]. These included number of involved lobes, extent of radiographic changes (<5%, 5%–25%, 25%–50%, and > 50%), distribution

of pneumonitis changes (focal vs. multifocal), specific CT findings (GGO, consolidation, or centrilobular nodularity), and radiographic patterns (COP, hypersensitivity pneumonitis, fibrosis, or AIP/ARDS). Sharp border, or the presence of a sharply demarcated linear edge between areas of pneumonitis and normal lung, is common among RT-pneumonitis [22, 23]. Therefore, the presence or absence of sharp border was also scored as an additional morphologic feature.

Statistical Analysis

Baseline patient and treatment characteristics were presented as number (percent) for categorical variables or median (range) for continuous variables. Comparisons between different treatment groups or pneumonitis severities were made by Fisher's exact test (categorical variables) or Wilcoxon rank sum test (continuous variables). CT morphologic features of RT- versus ICI-pneumonitis were compared using Fisher's exact tests. Statistical significance was defined as $p < .05$.

Radiomics and Machine Learning

We explored the feasibility of classifying pneumonitis etiology using radiomic features by training and validating a preliminary ML model. The bilateral whole lungs were automatically segmented using Velocity AI software (version 3.1, Varian, Palo Alto, CA) and shrunk by 3 mm isotropically to avoid partial volume effect at air-soft tissue interface. Ninety-three radiomic features (supplemental online Table 2) were extracted for each of the ipsilateral (relative to the primary tumor), contralateral and combined lungs from the pretreatment and post-treatment (at the time of pneumonitis) CT scans using PyRadiomics software (version 3.0 https://pyradiomics.readthedocs.io/) [24]. Feature selection was performed in a two-step process: first, t tests were used to compare RT- and ICI-pneumonitis, and the radiomic features with $p < .05$ were entered into the next step. Second, an iterative least absolute shrinkage and selection operator process with one feature left out in each iteration was used to select the final features (retained in more than one third of all iterations) [25]. Random forest algorithm was used for model training in patients who received RT ($n = 29$) or ICI ($n = 23$) alone. Hyperparameters were optimized via grid search, including the number of features used for splitting at each node (search grid: 1 to 10 with a step size of 1) and the number of trees (search grid: 200, 500, 1,000, 2,000, 5,000, 10,000).

The final model was tested in the group of patients receiving RT + ICI. The model yielded the likelihood of ICI being the predominant etiology (on a continuous scale of 0, least likely, to 1, most likely) in each case. As no gold standard exists to definitively distinguish pneumonitis etiology in this patient population, we compared the results from the model with the consensus attribution by a multidisciplinary group of physicians consisting of both radiation oncologists and medical oncologists with access to all the clinical and imaging records. All predictive modeling was performed using R software.

RESULTS

Patient Characteristics

Baseline patient characteristics are summarized in Table 1. Eighty-two patients were included in this study, with a median follow-up of 15.4 months (range, 0.7–129.6). The median patient age was 68 years (range, 45–84), and 50% were male. Thirteen patients (16%) were current smokers and 57 (70%) were former smokers, with a median of 35 pack-year smoking history (range, 1–110). Thirty-eight patients (46%) had prior diagnosis of COPD. Two patients had a history of interstitial lung disease (ILD): one had stable subpleural fibrosis on CT consistent with ILD prior to initiating ICI, and the other had an episode of bronchiolitis obliterans organizing pneumonia 7 years prior to diagnosis and received RT and ICI after lung cancer diagnosis. Neither patient was taking corticosteroids at the time of initiating lung cancer treatment.

Baseline characteristics, including age, gender, performance status, smoking history, pre-existing COPD diagnosis, pretreatment lung function, and tumor T and N stages were similar among patients who received RT alone, ICI alone and RT + ICI. Patients in the ICI alone group compared with the RT alone or RT + ICI alone group had lower median pack-year smoking history (25 vs. 40 for RT alone and 38 for RT + ICI; $p = .02$), higher proportion of adenocarcinoma histology (83% vs. 55% for RT alone and 43% for RT + ICI; $p = .04$), and higher proportion of metastatic disease at the time of initial diagnosis (83% vs. 7% for RT alone and 20% for RT + ICI; $p < .001$). The majority of patients in the RT alone (86%) and RT + ICI (63%) groups had stage III disease, whereas the majority of patients in the ICI alone group were stage IV (83%).

Treatment Characteristics

RT and ICI treatment characteristics are summarized in Table 2. All thoracic RT treatments were delivered using intensity-modulated radiotherapy to a median dose of 62 Gy (range, 45–72). The median lung V20 was 25% (range, 14%–41%), and the median MLD was 15.0 Gy (range, 8.6–21.7 Gy). RT doses to the normal lungs were lower in the RT + ICI group compared with the RT alone group (Table 1; median lung V20, 24% vs. 28%; $p = .03$; MLD: 13.5 vs. 16.1 Gy; $p = .02$). This may be related to improvement in treatment planning, as the majority of patients who received RT alone (59%) completed RT in or before the year 2014, whereas the majority in the RT + ICI group completed RT after 2014 (70%).

Patients who received ICI were treated with a variety of agents, including nivolumab (55%), durvalumab (21%), pembrolizumab (11%), or a combination of ipilimumab and nivolumab (13%). All patients in the RT + ICI group initiated ICI after completion of RT. The median time from RT completion to ICI initiation was 4.5 months (range, 0.4–48.1). Among patients who received ICI alone, 83% were treated with an anti–programmed death 1 (PD-1; nivolumab or pembrolizumab) and 17% received combined anti–cytotoxic T-lymphocyte antigen 4 (CTLA-4)/PD-1 antibodies. In contrast, 53% of patients in the RT + ICI group received an

Table 1. Baseline patient characteristics

Characteristics	RT alone	ICI alone	RT + ICI	p value
Number of patients	29	23	30	
Age, yr[a]	67 (45–84)	65 (50–81)	69 (49–82)	.57
Male, n (%)	12 (41)	11 (48)	18 (60)	.35
ECOG performance status (%)				.38
0	6 (21)	3 (13)	5 (17)	
1	23 (79)	17 (74)	22 (73)	
2	0	3 (13)	3 (10)	
Smoking history, n (%)				.26
Current smoker	2 (7)	3 (13)	8 (27)	
Former smoker	23 (79)	15 (65)	19 (63)	
Never smoker	4 (14)	5 (22)	3 (10)	
Pack-year smoked[a]	40 (0–90)	25 (0–90)	38 (0–110)	.02
COPD (%)	16 (55)	8 (35)	14 (47)	.34
Autoimmune disease (%)				.91
ILD	0	1 (4)	1 (3)	
Crohn's disease	1 (3)	0	0	
Rheumatoid arthritis	1 (3)	0	0	
Myasthenia gravis	0	0	1 (3)	
Pretreatment lung function[a]				
FEV1, L	1.46 (1.10–1.99)	1.93 (1.40–2.69)	1.87 (1.50–2.25)	.29
% FEV1 predicted	74 (39–84)	76 (64–90)	74 (56–84)	.47
FVC, L	2.41 (1.72–3.06)	2.68 (2.29–3.69)	2.88 (2.24–3.75)	.56
% FVC predicted	80 (56–102)	87 (78–100)	94 (66–99)	.64
DLCO (%)	54 (51–66)	85 (60–96)	80 (62–97)	.05
Histology (%)				.04
Adenocarcinoma	16 (55)	19 (83)	13 (43)	
Squamous cell carcinoma	8 (28)	3 (13)	13 (43)	
Other[b]	5 (17)	1 (4)	4 (13)	
T stage (%)				.78
1	5 (17)	4 (17)	5 (17)	
2	10 (34)	9 (39)	8 (27)	
3	6 (21)	3 (13)	10 (33)	
4	8 (28)	7 (30)	7 (23)	
N stage, n (%)				.52
0	4 (14)	3 (13)	7 (23)	
1	2 (7)	2 (9)	6 (20)	
2	19 (66)	13 (56)	14 (47)	
3	4 (14)	5 (22)	3 (10)	
Metastatic disease (%)	2 (7)	19 (83)	6 (20)	<.001
Overall stage at diagnosis (%)				<.001
I	0	2 (9)	1 (3)	
II	2 (7)	1 (4)	4 (13)	
III	25 (86)	1 (4)	19 (63)	
IV	2 (7)	19 (83)	6 (20)	

[a]Continuous variables are presented as median (range).
[b]Other histologies included adenosquamous (n = 1), carcinoid (n = 1), large cell (n = 2), and poorly differentiated non-small cell lung cancer (n = 6).
Abbreviations: COPD, chronic obstructive pulmonary disease; DLCO, diffusing capacity for carbon monoxide; ECOG, Eastern Cooperative Oncology Group; FEV1, forced expiratory volume in 1 second; FVC, forced vital capacity; ICI, immune checkpoint inhibitor; ILD, interstitial lung disease; RT, radiotherapy.

Table 2. Treatment characteristics and clinical features of pneumonitis

Characteristics	RT alone	ICI alone	RT + ICI	p value
Number of patients	29	23	30	
Thoracic RT[a]				
Prescription dose (Gy)	61.2 (45–72)	NA	63 (52.5–66.6)	.57
Lung V20 (% total lung)	28 (17–41)	NA	24 (14–37)	.03
Mean lung dose (Gy)	16.1 (9.6–21.7)	NA	13.5 (8.6–18.9)	.02
ICI type (%)	NA			.01
Nivolumab	NA	16 (70)	13 (43)	
Pembrolizumab	NA	3 (13)	3 (10)	
Ipilimumab-Nivolumab	NA	4 (17)	3 (10)	
Durvalumab	NA	0	11 (37)	
Interval between RT and ICI, mo	NA	NA	4.5 (0.4–48.1)	NA
Other treatments, n (%)				
Chemotherapy	15 (65)	28 (97)	29 (97)	.001
Thoracic surgery	4 (17)	8 (28)	6 (20)	.67
Time to pneumonitis onset, mo[a]	3.1 (0.4–12.0)	2.7 (0.1–17.5)	1.2 (0.1–34.3)	.12
Pneumonitis grade (%)				.59
1	0	2 (9)	1 (3)	
2	19 (66)	12 (52)	19 (63)	
3	9 (31)	6 (26)	7 (23)	
4	1 (3)	3 (13)	3 (10)	

[a]Continuous variables are presented as median (range).

Abbreviations: ICI, immune checkpoint inhibitor; RT, radiotherapy; V20, volume of the lung receiving 20 Gy or higher.

anti–PD-1 antibody, 37% received anti–programmed death ligand 1 antibody (durvalumab), and 10% received combined anti–CTLA-4/PD-1 (Table 2).

Clinical Features of Pneumonitis

The median time to pneumonitis onset was 2.6 months (range, 0.1–34.3) in the entire cohort. There was a trend toward more rapid onset of pneumonitis in patients receiving RT + ICI (median time of onset 1.2 months, range 0.1–34.3), compared with patients who received RT (median onset 3.1 months, range 0.4–12.0) or ICI alone (median onset 2.7 months, range 0.1–17.5; p = .12). The majority of pneumonitis were grade 2 (61%) or grade 3 (27%). There was no significant difference in pneumonitis grades among the three groups (Table 2).

Morphologic Features of RT- Versus ICI-Pneumonitis

Figure 1 demonstrates representative CT images of RT- and ICI-pneumonitis. RT-pneumonitis often centered on the lung ipsilateral to the primary tumor and had sharp border (arrowheads) after RT alone (Fig. 1A). In contrast, ICI-pneumonitis was often bilateral, involving multiple lobes, and without sharp border in patients treated with ICIs alone (Fig. 1B). Among patients who received both RT and ICIs, some (Fig. 1C) were confined to the ipsilateral lung with sharp borders similar to RT-pneumonitis, while others (Fig. 1D) resembled the bilateral distribution of typical ICI-pneumonitis.

Table 3 summarizes the seven morphologic features of RT- and ICI-pneumonitis. In patients who developed ICI-pneumonitis after ICIs alone compared with patients who developed RT-pneumonitis after RT alone, ICI-pneumonitis was more likely bilateral (65 vs. 28%; p = .01), involved more lobes of the lung (66% vs. 45% involving three or more lobes; p = .02), and was less likely to have sharp border (17% vs. 59%; p = .004). There was a trend of ICI-pneumonitis involving greater volume of the lung (52% ICI vs. 45% RT involving ≥25% lung volume; p = .25). Specific CT elements (most commonly GGOs and/or consolidations) and radiographic patterns (most commonly AIP/ARDS or COP) were not significantly different between RT- and ICI-pneumonitis.

In aggregate, pneumonitis CT morphology in the RT + ICI group had features of both RT-pneumonitis and ICI-pneumonitis. Forty-seven percent of pneumonitis in the RT + ICI group was bilateral, 37% involved three or more lobes of the lung, 34% involved ≥25% lung volume, and 40% had sharp borders. Similar to RT-pneumonitis, pneumonitis after RT + ICI involved fewer lobes than ICI-pneumonitis (p = .01) and trended toward lower likelihood of bilateral involvement (p = .06), involving lower volume of the lung (p = .07) and higher likelihood of having sharp borders (p = .13) than pneumonitis from ICI alone.

Factors Associated with Higher-Grade Pneumonitis

To explore the clinical and morphologic features associated with pneumonitis severity, we performed univariable analyses by dichotomizing pneumonitis severity into lower grade (grade 1–2) and higher grade (grade 3–4, Table 4). In the entire cohort, patients with grade 3–4 pneumonitis had
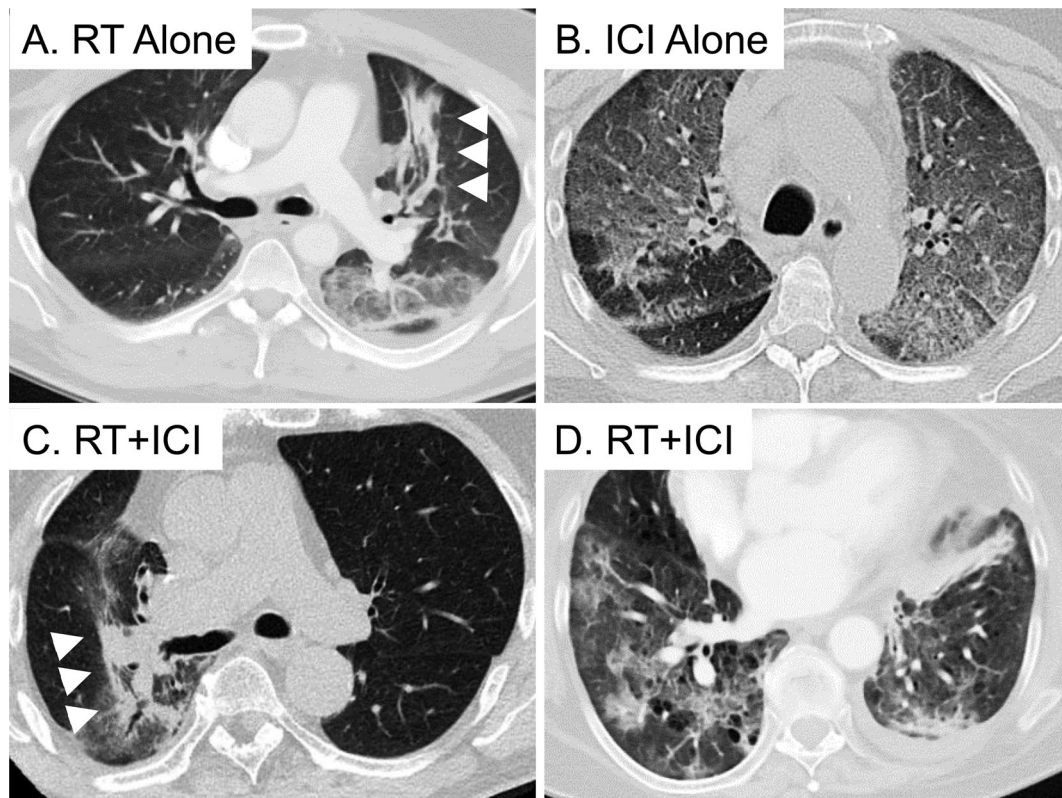
Figure 1. Representative computed tomography (CT) images of RT-pneumonitis **(A)**, ICI-pneumonitis **(B)**, and pneumonitis after RT + ICI **(C, D)**. **(A):** A 66-year-old patient with stage IIIA adenocarcinoma of the left upper lobe (LUL) developed RT-pneumonitis 1.4 months after completing thoracic RT. CT changes included focal consolidation with a sharp border (arrowheads) in the lung ipsilateral to the primary tumor. **(B):** A 68-year-old patient with a stage IV adenocarcinoma of the right lower lobe developed ICI-pneumonitis 3.7 months after initiating nivolumab. CT changes included bilateral, multifocal ground-glass opacities (GGOs) without sharp border. **(C):** A 68-year-old patient with stage IIIA adenocarcinoma of the right upper lobe developed RT-pneumonitis 2.6 months after completing RT and initiating durvalumab. CT changes included focal GGOs and consolidation with a sharp border (arrowheads) in the ipsilateral lung, resembling RT-pneumonitis. **(D):** A 62-year-old patient with stage IIIA squamous cell carcinoma of the LUL developed ICI-pneumonitis 0.8 months after completing RT and initiating durvalumab. CT changes included bilateral, multifocal GGOs without sharp border, resembling ICI-pneumonitis.
Abbreviations: ICI, immune checkpoint inhibitor; RT, radiotherapy.

worse baseline Eastern Cooperative Oncology Group performance score ($p = .01$), higher likelihood of being current or former smokers (100% vs. 77%; $p = .007$), higher pack-year smoking history (median 40 vs. 30 pack-years; $p = .03$), and lower FEV1 (median 1.48 vs. 1.94 L; $p = .03$; median 67% vs. 79% predicted; $p = .01$) and FVC (median 2.41 vs. 2.73 L; $p = .04$; median 79% vs. 91% predicted; $p = .03$) when compared with patients with grade 1–2 pneumonitis. In evaluating morphologic features among all patients, patients with grade 3–4 pneumonitis were more likely to have bilateral changes (62% vs. 24%; $p = .002$), multifocal involvement (97% vs. 60%; $p < .001$), involvement of three or more lobes (69% vs. 36%; $p = .006$), involvement of 25% or greater volume of the lung (69% vs. 28%; $p < .001$), demonstrating GGO component (76% vs. 45%; $p = .01$), and having an AIP/ARDS pattern (55% vs. 28%; $p = .01$) when compared with patients with grade 1–2 pneumonitis. Among the subset of patients who received both thoracic RT and ICIs, patients with grade 3–4 pneumonitis trended toward having more extensive smoking history (100% vs. 85% being current or former smokers; $p = .10$; median 50 vs. 32 pack-years smoked; $p = .14$), and were more likely

to have bilateral (60% vs. 20%; $p = .04$) and multifocal (100% vs. 60%; $p = .03$) CT changes compared with patients with grade 1–2 pneumonitis. Grade 3–4 pneumonitis was not associated with age, histology, stage, lung V20, MLD, or the type of ICI in either the overall cohort or the RT + ICI group.

Radiomics and Machine Learning
We developed an exploratory ML model to classify pneumonitis etiology based on quantitative radiomic features alone, without the input of CT morphologic features, prior RT field, or the timing of onset. Supplemental online Table 3 lists the seven radiomic features selected for the model. Similar to morphologic exams, pneumonitis after RT + ICI exhibited intermediate radiomic features compared with the RT alone and ICI alone groups. Two radiomic features were similar between pure RT-pneumonitis and pneumonitis after receipt of RT + ICI, which were significantly or near significantly different from ICI-pneumonitis. Conversely, four radiomic features were similar between pure ICI-pneumonitis and pneumonitis after receipt of RT + ICI, which were significantly or near significantly different

Table 3. Morphologic features of RT- versus ICI-pneumonitis

Features	RT alone	ICI alone	*p* value[a] (RT vs. ICI)	RT + ICI	*p* value[a] (RT + ICI vs. RT alone)	*p* value[a] (RT + ICI vs. ICI alone)
n	29	23		30		
Bilateral	8 (28)	15 (65)	.01	14 (47)	.57	.06
Number of lobes			.02		.87	.01
1	5 (17)	5 (22)		4 (13)		
2	11 (38)	3 (13)		15 (50)		
3	8 (28)	3 (13)		6 (20)		
4	3 (10)	2 (9)		2 (7)		
5	2 (7)	10 (44)		3 (10)		
Volume of lung involved			.25		.70	.07
<5%	2 (7)	3 (13)		1 (3)		
5%–25%	14 (48)	8 (35)		19 (63)		
25%–50%	10 (35)	6 (26)		8 (27)		
>50%	3 (10)	6 (26)		2 (7)		
Multifocal	21 (72)	17 (74)	.99	22 (73)	1.00	.99
Radiographic elements			.44		.31	.34
GGO	11 (38)	9 (39)		7 (23)		
Consolidation	12 (41)	10 (44)		11 (37)		
GGO + cons	6 (21)	3 (13)		10 (33)		
Nodules	0	1 (4)		2 (7)		
Radiographic pattern			.53		.50	.49
AIP/ARDS	12 (46)	11 (52)		8 (30)		
COP	12 (46)	8 (38)		14 (52)		
Fibrosis	2 (8)	0		2 (7)		
COP + fibrosis	0	1 (5)		1 (4)		
HP	0	1 (5)		2 (7)		
Sharp border	17 (59)	4 (17)	.004	12 (40)	.20	.13

Data are presented as *n* (%).
[a]*p* values from Fisher's exact tests.
Abbreviations: AIP/ARDS, acute interstitial pneumonia/acute respiratory distress syndrome; cons, consolidation; COP, cryptogenic organizing pneumonia; GGO, ground-glass opacity; HP, hypersensitivity pneumonitis; ICI, immune checkpoint inhibitor; RT, radiotherapy.

from RT-pneumonitis. Supplemental online Figure 1A–D demonstrates the differences in contralateral neighboring gray tone difference matrix (NGTDM) contrast in the same patients as Figure 1A–D. NGTDM contrast measures differences in CT density between each voxel and its surrounding voxels, and higher values suggest greater tissue heterogeneity and pathology [26, 27]. ICI-pneumonitis (supplemental online Fig. 1B) had higher NGTDM contrast values than RT-pneumonitis (supplemental online Fig. 1A), which was recapitulated by the difference between two patients with pneumonitis after RT + ICI (supplemental online Fig. 1D vs. 1C).

Figure 2A demonstrates the receiver-operating characteristics of the final ML model in the RT or ICI alone groups, with an area under the curve of 0.76 (95% confidence interval, 0.63–0.90). To test whether this model could identify the predominant etiology of pneumonitis after RT + ICI, we applied the ML model to the RT + ICI group of patients and compared the model prediction in each case to the attribution determined by the multidisciplinary consensus. As shown in Figure 2B, the height of each bar represents the likelihood of ICI being the predominant etiology of pneumonitis in each patient, as predicted by the ML model. The patients for whom ICI was the most likely etiology by consensus also tended to have higher likelihood predicted by the ML model (black bars clustering toward the right side of the graph), while those less likely to be caused by ICI (more likely RT) by consensus also had lower likelihood predicted by the model (gray bars clustering toward the left side of the graph).

DISCUSSION

To our knowledge, this is the first study in which pneumonitis due to different etiologies, including RT, ICI, and potentially combination of the two in patients who received

Table 4. Factors associated with higher-grade (grade 3–4) pneumonitis

Variables	Overall cohort			RT + ICI		
	Grade 1–2	Grade 3–4	p value	Grade 1–2	Grade 3–4	p value
n (%)	53 (65)	29 (35)		20 (67)	10 (33)	
Age[a]	69 (45–84)	68 (48–80)	.77	69 (56–82)	66 (49–77)	.57
ECOG performance score[b]			.01			.56
0	13 (24)	1 (3)		4 (20)	1 (10)	
1	38 (72)	24 (83)		15 (75)	7 (70)	
2	2 (4)	4 (14)		1 (5)	2 (20)	
Smoking history[b]			.007			.10
Current smoker	6 (11)	7 (24)		3 (15)	5 (50)	
Former smoker	35 (66)	22 (76)		14 (70)	5 (50)	
Never smoker	12 (23)	0		3 (15)	0	
Pack-year smoked[a]	30 (0–110)	40 (10–100)	.03	32 (0–110)	50 (10–100)	.14
History of autoimmune disease[a]	2 (4)	3 (10)	.37	1 (5)	1 (10)	.56
Pretreatment lung function[a]						
FEV1, L						.70
% FEV1 predicted						.38
FVC, L						.53
% FVC predicted						.53
Histology[a]			.84			.65
Adenocarcinoma	32 (60)	16 (55)		10 (50)	3 (30)	
Squamous cell carcinoma	15 (28)	9 (31)		8 (40)	5 (50)	
Other	6 (11)	4 (14)		2 (10)	2 (20)	
Initial stage[b]			.79			.44
I	3 (6)	0		1 (5)	0	
II	4 (8)	3 (10)		2 (10)	2 (20)	
III	29 (55)	16 (55)		12 (60)	7 (70)	
IV	17 (32)	10 (35)		5 (25)	1 (10)	
Radiation dosimetry[a]	(n = 39)	(n = 20)				
V20 (% total lung)	25 (17–41)	26 (14–35)	0.99	24 (17–37)	21 (14–32)	.67
MLD (Gy)	15.0 (8.9–21.7)	15.7 (8.6–20.0)	.56	13.2 (8.9–18.9)	15.0 (8.6–18.4)	.53
Type of ICI[b]	(n = 34)	(n = 19)	.74			.46
Nivolumab	17 (50)	12 (63)		9 (45)	4 (40)	
Pembrolizumab	5 (15)	1 (5)		3 (15)	0	
Ipilimumab-nivolumab	5 (15)	2 (11)		1 (5)	2 (20)	
Durvalumab	7 (20)	4 (21)		7 (35)	4 (40)	
Bilateral CT changes[b]	13 (24)	18 (62)	.002	4 (20)	6 (60)	.04
Multifocal CT changes[b]	32 (60)	28 (97)	<.001	12 (60)	10 (100)	.03
Involving three or more lobes[b]	19 (36)	20 (69)	.006	5 (25)	6 (60)	.11
Involving ≥25% lung volume[b]	15 (28)	20 (69)	<.001	5 (25)	5 (50)	.23
GGO component[b,c]	24 (45)	22 (76)	.01	10 (50)	7 (70)	.44
AIP/ARDS pattern[b]	15 (28)	16 (55)	.01	4 (20)	4 (40)	.18
Sharp border[b]	28 (53)	21 (72)	.10	13 (65)	5 (50)	.46

[a]Median (range). p values from Wilcoxon rank sum tests.
[b]Number of patients (%). p values from Fisher's exact tests.
[c]Including cases with GGO or GGO plus consolidations.
Abbreviations: AIP/ARDS, acute interstitial pneumonia/acute respiratory distress syndrome; ECOG, Eastern Cooperative Oncology Group; FEV1, forced expiratory volume in 1 second; FVC, forced vital capacity; GGO, ground-glass opacity; ICI, immune checkpoint inhibitor; MLD, mean lung dose; RT, radiotherapy; V20, volume of lung receiving at least 20 Gy.
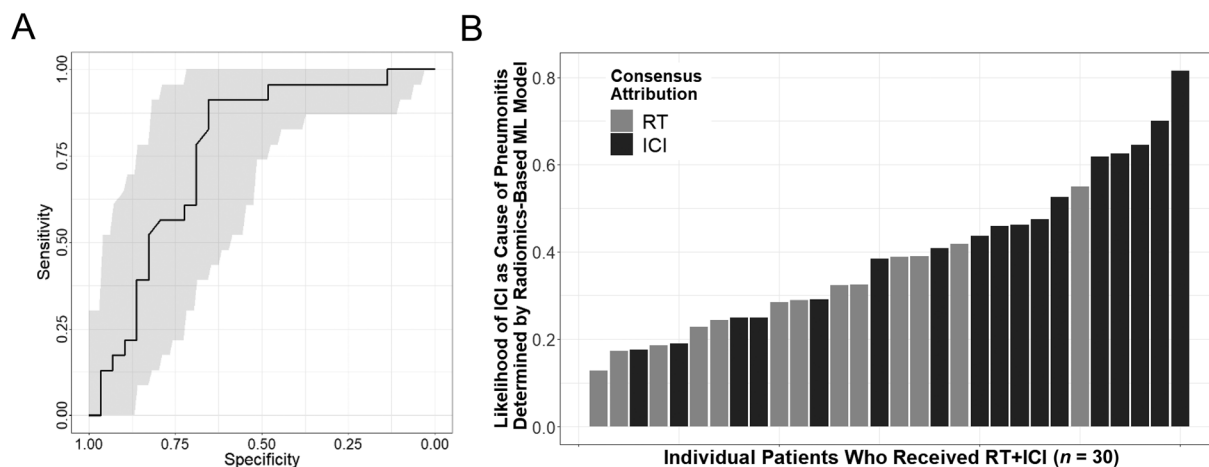
Figure 2. Radiomics-based machine learning model for distinguishing ICI- from RT-pneumonitis. **(A):** Receiver-operating characteristics (ROC) of the model in patients who received RT or ICI alone. The gray areas indicate 95% confidence intervals of the ROC. **(B):** Model prediction of the likelihood (least to most likely from 0 to 1) of ICI etiology in each patient (individual bars) who developed pneumonitis after RT + ICI ($n = 30$). The color of each bar represents the attribution by multidisciplinary consensus (gray for RT etiology, black for ICI etiology).
Abbreviations: ICI, immune checkpoint inhibitor; ML, machine learning; RT, radiotherapy.

both, are systematically compared. Our findings have potential implications in directing the treatment for pneumonitis in patients with NSCLC, as well as in understanding the pathogenesis of pneumonitis in patients who receive both RT and ICI. First, RT- and ICI-pneumonitis share similar CT elements (both commonly presenting as GGOs and/or consolidations) and patterns (often AIP/ARDS or COP) but differ in their spatial distribution in that ICI-pneumonitis tends to be bilateral, more likely to involve more lobes of the lung, and less likely to have sharp borders. Second, as a group, patients who develop pneumonitis after receipt of both RT and ICI exhibit an intermediate phenotype between RT- and ICI-pneumonitis in both morphologic and radiomic features, suggesting that both RT and ICI may contribute to the development of pneumonitis in this group. However, it should be noted that this is a heterogeneous group with some patients more closely resembling RT-pneumonitis and others ICI-pneumonitis (Fig. 1 and supplemental Fig. 1). Therefore, one etiology may play a more significant role in the development of pneumonitis than the other in a particular patient. The biologic underpinning of such differences in pneumonitis pathogenesis remains to be determined. Nevertheless, treatment of pneumonitis after RT + ICI may need to be individualized to take into account of the predominant etiology.

The number of patients who develop pneumonitis after RT and ICIs is increasing because of the expanding indications for both thoracic RT and ICIs in patients with NSCLC [7, 14, 28]. The incidence of pneumonitis in patients with locally advanced NSCLC after definitive chemoradiotherapy and ICIs may be as high as 34% [29]. The treatment algorithms and natural histories differ dramatically between RT- and ICI-pneumonitis. Patients with RT-pneumonitis are often treated with a lower dose of steroids (40–60 mg prednisone per day) for a shorter duration of time, whereas those with ICI-pneumonitis require high-dose steroids (1–2 mg prednisone per kg per day) for a prolonged period [13].

High-grade, steroid refractory ICI-pneumonitis can develop in as many as 18% of patients and may require intravenous immunoglobulin or other immunosuppressive agents such as mycophenolate mofetil or infliximab [13, 30]. In addition, patients with ICI-pneumonitis are at a higher risk of recrudescence when rechallenged with ICIs, while ICI rechallenge might be less problematic in patients whose pneumonitis is mainly due to RT [31]. Therefore, identifying the predominant etiology responsible for pneumonitis development after RT + ICI may help to triage patients toward the best treatment pathway.

Despite the clinical need to better define pneumonitis etiology, there is no consensus to guide the distinction of pneumonitis etiology after receipt of both RT and ICIs. Traditional clinical factors, such as the timing of onset and RT dose distribution are two of the most commonly used criteria, but it requires multidisciplinary input from all members of the treatment team, and the results can still be ambiguous in many cases [9, 12]. In our own cohort, initial classification of pneumonitis etiology by two of the authors was only concordant in 63% of cases, even with the full medical, imaging, and treatment history available, which may be partly due to contributions from both RT and ICIs in pneumonitis development. The morphologic features identified in this study, namely laterality, number of lobes involved, and sharp border, may help refine the attribution of the predominant pneumonitis etiology in patients receiving RT + ICI, thereby facilitating treatment decision-making in this patient population.

Radiomics and ML may play an increasingly active role in assisting human readers and evaluating CT scans in patients with NSCLC. Our results demonstrate the feasibility of using unbiased radiomic features, instead of qualitative morphologic features, to distinguish pneumonitis etiology. Previous studies have shown promising results of radiomics in predicting pneumonitis risk after RT or ICI [18–21]. However, these studies did not differentiate between RT- and

ICI-pneumonitis and did not include patients treated with RT + ICI. In this study, we identified high post-treatment NGTDM contrast in the contralateral lung as a potential biomarker for ICI-pneumonitis. NGTDM contrast may help differentiate normal versus malignant tissues and predict treatment response in NSCLC, head and neck cancer, rectal cancer, and multiple myeloma [26, 27, 32–34]. Interestingly, in a retrospective study of 43 patients with triple-negative breast cancer, higher NGTDM contrast on mammography was associated with a higher number of tumor-infiltrating lymphocytes [27]. Lymphocytes are central to the pathogenesis of ICI-pneumonitis. The link between NGTDM contrast and lymphocyte infiltration may provide a plausible mechanism for the morphologic findings of pneumonitis after ICIs or RT + ICI [35, 36].

This study also contributes to our understanding of the risk factors for severe pneumonitis. Grade 3–4 pneumonitis was associated with worse baseline performance status, greater smoking history, and lower pretreatment lung function, in particular, FEV1 and FVC. This is consistent with previous findings that pretreatment FEV1 is associated with severe radiation pneumonitis [5, 37]. Radiation dose to the lung, in particular V20 and MLD, were not associated with pneumonitis severity in our cohort of patients who received RT or RT + ICI, possibly because of the small sample size and heterogeneity in disease stage. Among the imaging features, bilateral and multifocal involvement were significantly associated with severe pneumonitis in both the overall cohort and among patients who received RT + ICI. Similarly, previous studies have identified bilateral involvement as a risk factor for both fatal RT-pneumonitis and steroid refractory ICI-pneumonitis [30, 38]. These clinical and imaging risk factors may assist in the identification of patients with NSCLC with pneumonitis who may be at high risk of clinical deterioration and may require treatment intensification for pneumonitis.

The main caveat of this study is the small cohort size. However, the size of our study population is on par with previous reports in this area [3, 5, 9]. As such, we were not able to perform multivariable analysis on the risk factors for higher-grade pneumonitis because of the small sample size. Future prospective studies with larger patient cohorts should be conducted to independently validate the imaging biomarkers and risk factors identified in this study. Further research is also needed to better characterize the temporal evolution of the imaging findings of pneumonitis, which may serve as early biomarkers for patients who are at risk of clinical deterioration and may require escalation of pneumonitis treatments. Finally, mechanistic studies combining imaging and serum biomarkers, such as interleukin-8 and chemotactic cytokine ligand 2, may elucidate the underlying etiology of pneumonitis after RT + ICI and identify novel therapeutic targets [39–43].

Conclusion

In a cohort of patients with NSCLC treated with definitive dose of thoracic RT and/or ICIs, RT-pneumonitis is more likely to be unilateral, involve fewer lobes of the lung, and have sharp border, whereas ICI-pneumonitis tends to be bilateral and involve more lobes and is less likely to have sharp border. Patients who develop pneumonitis after both RT and ICI have heterogeneous morphologic presentations, with features overlapping with both RT- and ICI-pneumonitis. Poor performance status, greater smoking history, lower pretreatment lung function, and bilateral and multifocal involvement on CT are risk factors associated with severe pneumonitis. Lastly, an exploratory radiomics-based ML model can identify the predominant pneumonitis etiology in patients who received RT + ICI with good concordance with the clinical impression of a multidisciplinary group of physicians. Future studies with larger patient cohorts are needed to validate these findings.

Author Contributions

Conception/design: Xuguang Chen, Khinh Ranh Voong
Provision of study material or patients: Russell K. Hales, Patrick M. Forde, Jarushka Naidoo, Khinh Ranh Voong
Collection and/or assembly of data: Xuguang Chen, Khadija Sheikh, Erica Nakajima, Cheng Ting Lin, Junghoon Lee
Data analysis and interpretation: Xuguang Chen, Khadija Sheikh, Cheng Ting Lin, Chen Hu
Manuscript writing: Xuguang Chen, Khinh Ranh Voong
Final approval of manuscript: Xuguang Chen, Khadija Sheikh, Erica Nakajima, Cheng Ting Lin, Junghoon Lee, Chen Hu, Russell K. Hales, Patrick M. Forde, Jarushka Naidoo, Khinh Ranh Voong

References

1. Ko EC, Raben D, Formenti SC. The integration of radiotherapy with immunotherapy for the treatment of non-small cell lung cancer. Clin Cancer Res 2018;24:5792–5806.

2. Li M, Gan L, Song A et al. Rethinking pulmonary toxicity in advanced non-small cell lung cancer in the era of combining anti-PD-1/PD-L1 therapy with thoracic radiotherapy. Biochim Biophys Acta Rev Cancer 2019; 1871:323–330.

3. Nishino M, Ramaiya NH, Awad MM et al. PD-1 inhibitor-related pneumonitis in advanced cancer patients: Radiographic patterns and clinical course. Clin Cancer Res 2016;22:6051–6060.

4. Naidoo J, Wang X, Woo KM et al. Pneumonitis in patients treated with anti-programmed death-1/programmed death ligand 1 therapy. J Clin Oncol 2017;35:709–717.

5. Thomas R, Chen YH, Hatabu H et al. Radiographic patterns of symptomatic radiation pneumonitis in lung cancer patients: Imaging

predictors for clinical severity and outcome. Lung Cancer 2020;145:132–139.

6. Gomez DR, Blumenschein GR Jr, Lee JJ et al. Local consolidative therapy versus maintenance therapy or observation for patients with oligometastatic non-small-cell lung cancer without progression after first-line systemic therapy: A multicentre, randomised, controlled, phase 2 study. Lancet Oncol 2016;17:1672–1682.

7. Friedes C, Mai N, Hazell S et al. Consolidative radiotherapy in oligometastatic lung cancer: Patient selection with a prediction nomogram. Clin Lung Cancer 2020;21:e622–e632.

8. Voong KR, Hazell SZ, Fu W et al. Relationship between prior radiotherapy and checkpoint-inhibitor pneumonitis in patients with advanced non-small-cell lung cancer. Clin Lung Cancer 2019;20:e470–e479.

9. Cousin F, Desir C, Ben Mustapha S et al. Incidence, risk factors, and CT characteristics of radiation recall pneumonitis induced by immune checkpoint inhibitor in lung cancer. Radiother Oncol 2021;157:47–55.

10. Barrón F, Sánchez R, Arroyo-Hernández M et al. Risk of developing checkpoint immune pneumonitis and its effect on overall survival in non-small cell lung cancer patients previously treated with radiotherapy. Front Oncol 2020;10:570233.

11. Park H, Hatabu H, Ricciuti B et al. Immune-related adverse events on body CT in patients with small-cell lung cancer treated with immune-checkpoint inhibitors. Eur J Radiol 2020;132:109275.

12. Voong KR, Naidoo J. Radiation pneumonitis after definitive chemoradiation and durvalumab for non-small cell lung cancer. Lung Cancer 2020;150:249–251.

13. Darnell EP, Mooradian MJ, Baruch EN et al. Immune-related adverse events (irAEs): Diagnosis, management, and clinical pearls. Curr Oncol Rep 2020;22:39.

14. Antonia SJ, Villegas A, Daniel D et al. Overall survival with durvalumab after chemoradiotherapy in stage III NSCLC. N Engl J Med 2018;379:2342–2350.

15. Brahmer J, Reckamp KL, Baas P et al. Nivolumab versus docetaxel in advanced squamous-cell non-small-cell lung cancer. N Engl J Med 2015;373:123–135.

16. Lambin P, Leijenaar RTH, Deist TM et al. Radiomics: The bridge between medical imaging and personalized medicine. Nat Rev Clin Oncol 2017;14:749–762.

17. Kocher M, Ruge MI, Galldiks N et al. Applications of radiomics and machine learning for radiotherapy of malignant brain tumors. Strahlenther Onkol 2020;196:856–867.

18. Colen RR, Fujii T, Bilen MA et al. Radiomics to predict immunotherapy-induced pneumonitis: Proof of concept. Invest New Drugs 2018;36:601–607.

19. Cunliffe A, Armato SG, Castillo R et al. Lung texture in serial thoracic computed tomography scans: Correlation of radiomics-based features with radiation therapy dose and radiation pneumonitis development. Int J Radiat Oncol Biol Phys 2015;91:1048–1056.

20. Luna JM, Chao HH, Diffenderfer ES et al. Predicting radiation pneumonitis in locally advanced stage II-III non-small cell lung cancer using machine learning. Radiother Oncol 2019;133:106–112.

21. Moran A, Daly ME, Yip SSF et al. Radiomics-based assessment of radiation-induced lung injury after stereotactic body radiotherapy. Clin Lung Cancer 2017;18:e425–e431.

22. Park KJ, Chung JY, Chun MS et al. Radiation-induced lung disease and the impact of radiation methods on imaging features. Radiographics 2000;20:83–98.

23. Choi YW, Munden RF, Erasmus JJ et al. Effects of radiation therapy on the lung: Radiologic appearances and differential diagnosis. Radiographics 2004;24:985–997; discussion 998.

24. van Griethuysen JJM, Fedorov A, Parmar C et al. Computational radiomics system to decode the radiographic phenotype. Cancer Res 2017;77:e104–e107.

25. Sheikh K, Lee SH, Cheng Z et al. Predicting acute radiation induced xerostomia in head and neck cancer using MR and CT Radiomics of parotid and submandibular glands. Radiat Oncol 2019;14:131.

26. Yu H, Caldwell C, Mah K et al. Coregistered FDG PET/CT-based textural characterization of head and neck cancer for radiation treatment planning. IEEE Trans Med Imaging 2009;28:374–383.

27. Yu H, Meng X, Chen H et al. Correlation between mammographic radiomics features and the level of tumor-infiltrating lymphocytes in patients with triple-negative breast cancer. Front Oncol 2020;10:412.

28. Gomez DR, Tang C, Zhang J et al. Local consolidative therapy vs. maintenance therapy or observation for patients with oligometastatic non-small-cell lung cancer: Long-term results of a multi-institutional, phase II, randomized study. J Clin Oncol 2019;37:1558–1565.

29. Antonia SJ, Villegas A, Daniel D et al. Durvalumab after chemoradiotherapy in stage III non-small-cell lung cancer. N Engl J Med 2017;377:1919–1929.

30. Balaji A, Hsu M, Lin CT et al. Steroid-refractory PD-(L)1 pneumonitis: Incidence, clinical features, treatment, and outcomes. J Immunother Cancer 2021;9:e001731.

31. Dolladille C, Ederhy S, Sassier M et al. Immune checkpoint inhibitor rechallenge after immune-related adverse events in patients with cancer. JAMA Oncol 2020;6:865–871.

32. Lovinfosse P, Polus M, Van Daele D et al. FDG PET/CT radiomics for predicting the outcome of locally advanced rectal cancer. Eur J Nucl Med Mol Imaging 2018;45:365–375.

33. Chen S, Harmon S, Perk T et al. Using neighborhood gray tone difference matrix texture features on dual time point PET/CT images to differentiate malignant from benign FDG-avid solitary pulmonary nodules. Cancer Imaging 2019;19:56.

34. Ekert K, Hinterleitner C, Baumgartner K et al. Extended texture analysis of non-enhanced whole-body MRI image data for response assessment in multiple myeloma patients undergoing systemic therapy. Cancers (Basel) 2020;12:761.

35. Suresh K, Naidoo J, Zhong Q et al. The alveolar immune cell landscape is dysregulated in checkpoint inhibitor pneumonitis. J Clin Invest 2019;129:4305–4315.

36. Reuss JE, Suresh K, Naidoo J. Checkpoint inhibitor pneumonitis: Mechanisms, characteristics, management strategies, and beyond. Curr Oncol Rep 2020;22:56.

37. Robnett TJ, Machtay M, Vines EF et al. Factors predicting severe radiation pneumonitis in patients receiving definitive chemoradiation for lung cancer. Int J Radiat Oncol Biol Phys 2000;48:89–94.

38. Keffer S, Guy CL, Weiss E. Fatal radiation pneumonitis: Literature review and case series. Adv Radiat Oncol 2019;5:238–249.

39. Petit SF, van Elmpt WJ, Oberije CJ et al. [^{18}F]fluorodeoxyglucose uptake patterns in lung before radiotherapy identify areas more susceptible to radiation-induced lung toxicity in non-small-cell lung cancer patients. Int J Radiat Oncol Biol Phys 2011;81:698–705.

40. Castillo R, Pham N, Ansari S et al. Pre-radiotherapy FDG PET predicts radiation pneumonitis in lung cancer. Radiat Oncol 2014;9:74.

41. Chaudhuri AA, Binkley MS, Rigdon J et al. Pre-treatment non-target lung FDG-PET uptake predicts symptomatic radiation pneumonitis following Stereotactic Ablative Radiotherapy (SABR). Radiother Oncol 2016;119:454–460.

42. Yue J, McKeever M, Sio TT et al. Association of lung fluorodeoxyglucose uptake with radiation pneumonitis after concurrent chemoradiation for non-small cell lung cancer. Clin Transl Radiat Oncol 2017;4:1–7.

43. Yu H, Wu H, Wang W et al. Machine learning to build and validate a model for radiation pneumonitis prediction in patients with non-small cell lung cancer. Clin Cancer Res 2019;25:4343–4350.

See http://www.TheOncologist.com for supplemental material available online.